

## Biomatter



ISSN: (Print) 2159-2535 (Online) Journal homepage: <http://www.tandfonline.com/loi/kbim20>

# Role of culture conditions on in vitro transformation and cellular colonization of biomimetic HA-Col scaffolds

Doris M. Campos, Gloria A. Soares & Karine Anselme

To cite this article: Doris M. Campos, Gloria A. Soares & Karine Anselme (2013) Role of culture conditions on in vitro transformation and cellular colonization of biomimetic HA-Col scaffolds, *Biomatter*, 3:2, e24922, DOI: [10.4161/biom.24922](https://doi.org/10.4161/biom.24922)

To link to this article: <https://doi.org/10.4161/biom.24922>



Copyright © 2013 Landes Bioscience



Published online: 01 Apr 2013.



Submit your article to this journal [↗](#)



Article views: 152



View related articles [↗](#)



Citing articles: 7 View citing articles [↗](#)

# Role of culture conditions on in vitro transformation and cellular colonization of biomimetic HA-Col scaffolds

Doris M. Campos,<sup>1,2</sup> Gloria A. Soares<sup>1</sup> and Karine Anselme<sup>2,\*</sup>

<sup>1</sup>Department of Metallurgical and Materials Engineering; Federal University of Rio de Janeiro; Rio de Janeiro, Brazil; <sup>2</sup>Institut de Science des Materiaux de Mulhouse (IS2M); CNRS UMR7361; Université de Haute-Alsace; Mulhouse, France

**Keywords:** scaffold, colonization, dynamic culture, hydroxyapatite, collagen, porosity, stromal osteoprogenitor cells

We have recently developed new 3D hydroxyapatite/collagen (50/50 wt%) scaffolds using a biomimetic synthesis approach. The first in vitro tests performed in static culture showed a limited cell colonization and survival inside the scaffolds. The current study evaluated in dynamic culture the scaffold changes and colonization by human immortalized osteoprogenitor STRO-1A cells. The stability of our scaffolds in the different culture conditions (static, low flow, high flow) was validated by the maintenance of the pore diameter and interconnectivity over 21 d. The colonization and the viability of STRO-1A cells inside the scaffolds were further evaluated on histological sections. It was demonstrated that only the high flow-rate allowed cell survival after 7 d and a complete scaffold colonization. Moreover, the colonization and viability were different in function of the scaffold position inside the perfusion container. The differentiation markers (alkaline phosphatase activity, type I procollagen and osteocalcin synthesis) of STRO-1A cells were analyzed in the culture medium after 7, 14 and 21 d. The low flow-rate increased significantly the three markers compared with static conditions. In contrast, markers were reduced in high flow-rate compared with low flow-rate. To explain this surprising result, we hypothesized that the different molecules were actually adsorbed on the scaffold because of the closed circuit used in the high flow-rate conditions. In summary, this study provides original results on the influence of flow rate but mostly of the circuit used (open/closed) on the structural modifications and cell colonization of collagen-HA scaffolds.

## Introduction

Designed porous materials have been proposed as scaffolds for regenerative medicine applications. In particular, composites associating collagen and calcium phosphate have been tested for bone replacement and have shown good efficiency in vitro and in vivo.<sup>1-3</sup> We have recently developed new 3D hydroxyapatite/collagen (50/50 wt.%) scaffolds using a biomimetic synthesis approach.<sup>4</sup> The first in vitro biocompatibility tests we performed in static culture conditions showed a limited cell colonization and survival inside the scaffolds.<sup>4</sup> Dynamic culture systems are known to improve nutrient delivery and waste removal from 3D culture in porous scaffolds.<sup>5</sup> In particular, flow perfusion bioreactor systems are now considered to be the most valuable for bone tissue engineering.<sup>6</sup> Their efficiency is based not only on the higher nutrients and oxygen diffusion they permit to the center of the scaffold but also on the mechanical stimulation by shear stress that they apply on bone cells. A lot of custom-made perfusion systems have been developed but they cannot easily be compared.<sup>7-11</sup> Several perfusion systems were supplied by various manufacturers. In this paper, we chose a perfusion

container provided by Minucells and Minutissue™ (Bad Abbach, Germany) that allows perfusion of up to six scaffolds in parallel. This perfusion system is based on an open circuit meaning that the container is connected to a medium bottle (input) and to a waste reservoir (output) by gas-permeable silicon tubes. Improved in vitro bone-marrow-derived osteoblastic cells growth has been obtained previously with this system in porous ceramic materials<sup>12,13</sup> or on 2D membranes of biomimetically mineralised type I collagen.<sup>14</sup> Herein, the perfusion container was used as provided even if Volkmer et al. have shown that modifying this set-up to avoid circulation of medium around the scaffolds improved the cell survival inside the samples.<sup>15</sup> The flow rate has an important role in the mechanical stimulation by shear stress of cells but also for renewing nutrients inside the scaffolds.<sup>16,17</sup> The perfusion container tested herein was previously used with a medium flow of 1 mL/h<sup>14,15</sup> or 2 mL/h.<sup>12,13</sup> In order to evaluate the influence of flow rate on the colonization and growth of cells inside our scaffolds, two different medium flows (2 mL/h and 20 mL/h) were tested in our study. For the low flow, the open circuit was maintained although it was closed for the high flow due to medium cost. In this study, we not only investigated the influence of flow rate

\*Correspondence to: Karine Anselme; Email: karine.anselme@uha.fr

Submitted: 01/09/13; Revised: 03/28/13; Accepted: 05/03/13

Citation: Campos D, Soares G, Anselme K. Role of culture conditions on in vitro transformation and cellular colonization of biomimetic HA-Col scaffolds. Biomatter 2013; 3:e24922; <http://dx.doi.org/10.4161/biom.24922>

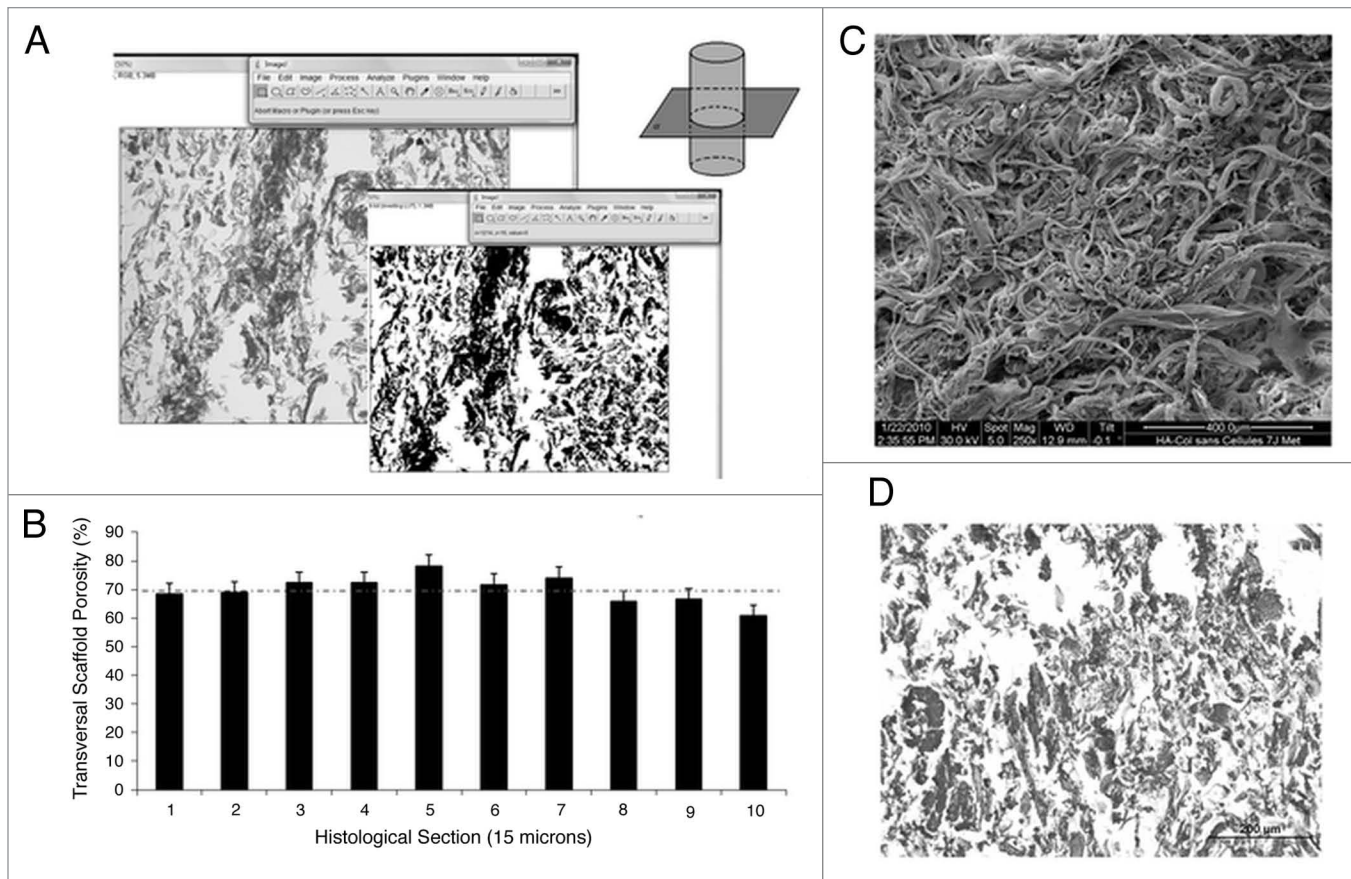


**Figure 1.** (A) A schematic diagram of the image treatment method to calculate the scaffold porosity on transversal sections; (B) Scaffold porosity on ten successive transversal sections; (C) SEM micrograph of HA-Col scaffold surface; (D) Histological cross-section of HA-Col scaffold stained by Picrosirius.

but also of the circuit used (open/closed) on the structural modifications and osteoprogenitor cell colonization of HA-collagen scaffolds.

## Results

**HA-Col scaffold characterization. Scaffold porosity.** HA-Col scaffolds prepared by self-assembly method showed an irregular porous and fibrous structure (Fig. 1). The scaffold porosity percentage and pore width were measured in order to verify the ability of these scaffolds to be colonised by cells. A homogenous porosity of 65–70% in the entire scaffold was measured from histological transversal cross-sections (Fig. 1A-B) and confirmed by liquid displacement measurements that gave 62% (v/v) of scaffold permeability. By image treatment, average pore diameters presented a heterogeneous distribution with a mean of  $280 \pm 80 \mu\text{m}$  (Fig. 1D).

**HA-Col scaffold stability.** The scaffold stability in static culture conditions was observed by SEM for up to 21 d. No morphological changes in structural parameters such as collagen fibers density, mineralization and scaffold global shape (Fig. 2A, B and C) were observed. The scaffold porosity measured on longitudinal sections was relatively stable even with the application of

mechanical forces due to fluid flow (Fig. 2D). Higher porosity could be observed in scaffolds submitted to high flow-rate (except at 7 d).

**HA-Col scaffold colonization. Cell colonization.** First, histological sections were analyzed in order to determine the total number of STRO-1A cell nuclei inside each sample. No significant differences were found in the number of cell nuclei per section after 1 and 3 d of culture in all culture conditions (Fig. 3). A lower quantity of cell nuclei was observed in scaffolds cultured for 24 h under high flow-rate. It seems that the dynamic high flow-rate was able to induce a cell detachment after 24 h in spite of the maintenance of the samples during 24 h in static conditions after inoculation to permit cell adhesion. After the first week, significant differences appeared between the conditions. Cell nuclei number was significantly higher in scaffolds cultured under high flow-rate conditions for 7, 14 and 21 d compared with scaffolds cultured in the two other conditions. At 21 d, a significantly higher number of nuclei were observed in scaffolds cultured in static conditions than in low flow-rate conditions (Fig. 3).

Second, histological sections were analyzed in order to determine the distribution of STRO-1A cells inside each sample. All samples presented cells essentially at the scaffold's surface at the

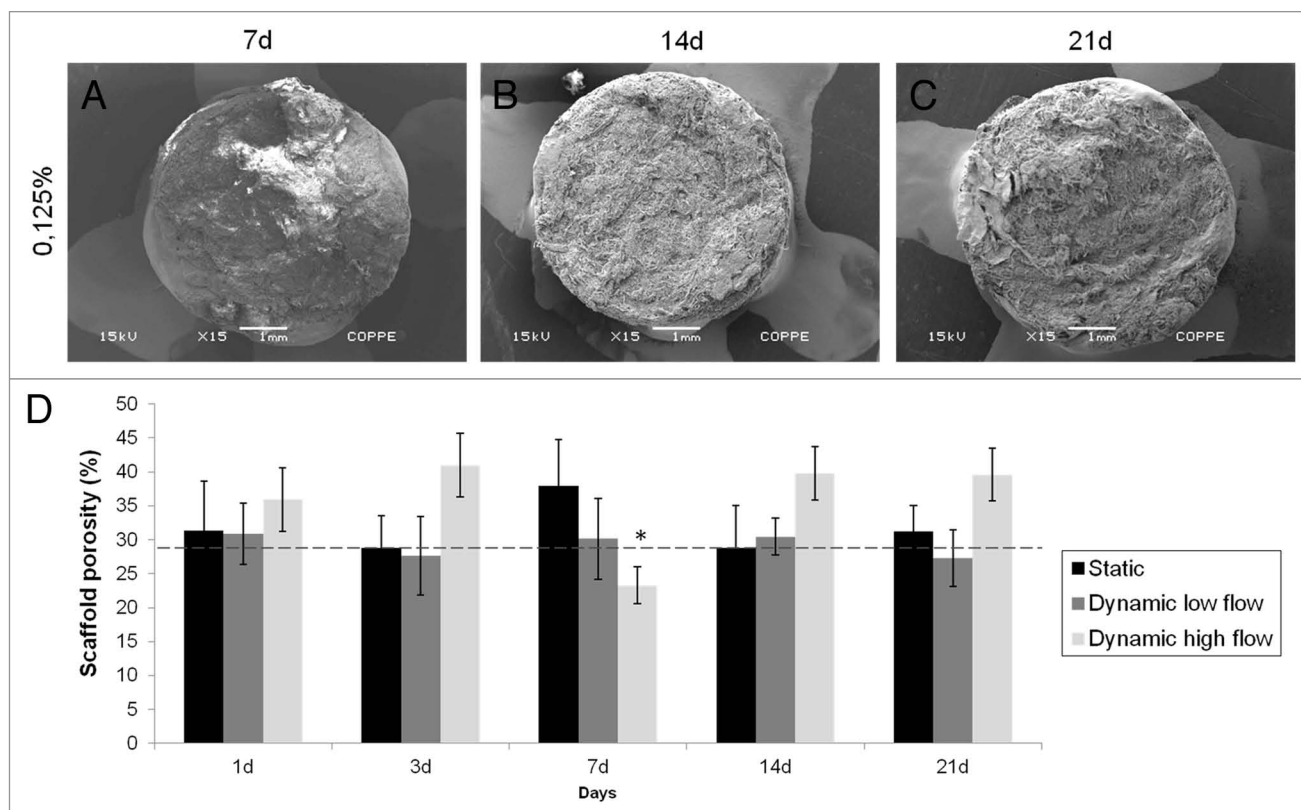


**Figure 2.** (A, B and C) SEM micrographs of scaffolds immersed under static culture condition up to 21 d and (D) total porosity of scaffolds maintained under different culture conditions up to 21 d. The dotted line indicates the initial porosity after 24 h under biological conditions. Error bars represent mean  $\pm$  SD with  $n = 4$ . The symbol (\*) indicates statistical significance within a timepoint ( $p < 0.01$ ).

initial time (data not shown). After 3 and 7 d, the fibrous and porous matrix of scaffolds facilitated cell migration and samples exhibited cell nuclei in the 100- $\mu$ m superficial layers for all culture conditions (data not shown). From 7 to 21 d of culture, the nuclei distribution inside the scaffolds varied significantly with culture conditions. Under static conditions, STRO-1A cells proliferated mainly at the periphery of samples and a monolayer of cell nuclei could be visualized on the scaffold surface after 21 d (Fig. 4A). Few cell nuclei were observed in the samples submitted to low flow-rate conditions (Fig. 4B) although a successful scaffold colonization was noted inside samples submitted to high flow-rate (Fig. 4C). The application of a high flow-rate also permitted cell proliferation in the center of the material while under low flow-rate, the proliferation process was not homogeneous inside the scaffolds. Cells proliferated more easily in the peripheral regions (Fig. 4E) than in the central ones (Fig. 4D). In order to interpret this behavior, a scheme of the liquid flow in the bioreactor was drawn (Fig. 4F).

**Cell viability.** Using the MTT assay, some significant differences in cell viability between the culture conditions were observed (Fig. 5A). Up to 7 d, an increase in the number of viable cells appeared in all conditions especially for both dynamic flow-rates. However, the cell viability decreased drastically from 7 d to 3 weeks under static and dynamic low-flow-rate culture conditions. Under high flow-rate conditions, the cells continued to proliferate and presented significantly higher cell viability at

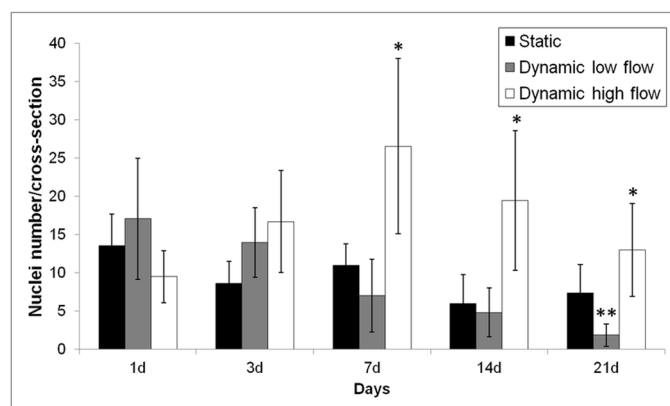


**Figure 3.** STRO-1A cell nuclei number stained by DAPI per longitudinal cross-section of HA-Col scaffolds cultured under different conditions up to 21 d. Error bars represent mean  $\pm$  SD with  $n = 4$ . The symbols (\*, \*\*) indicate statistical significance within a timepoint ( $p < 0.05$ ).

14 and 21 d when compared with static and low flow-rate conditions (Fig. 5A).

The number of viable cells was also analyzed considering the sample position in the bioreactor (Figs. 5B and C). When cells were submitted to low flow-rate conditions, sample position was shown to have an important role in the initial culture

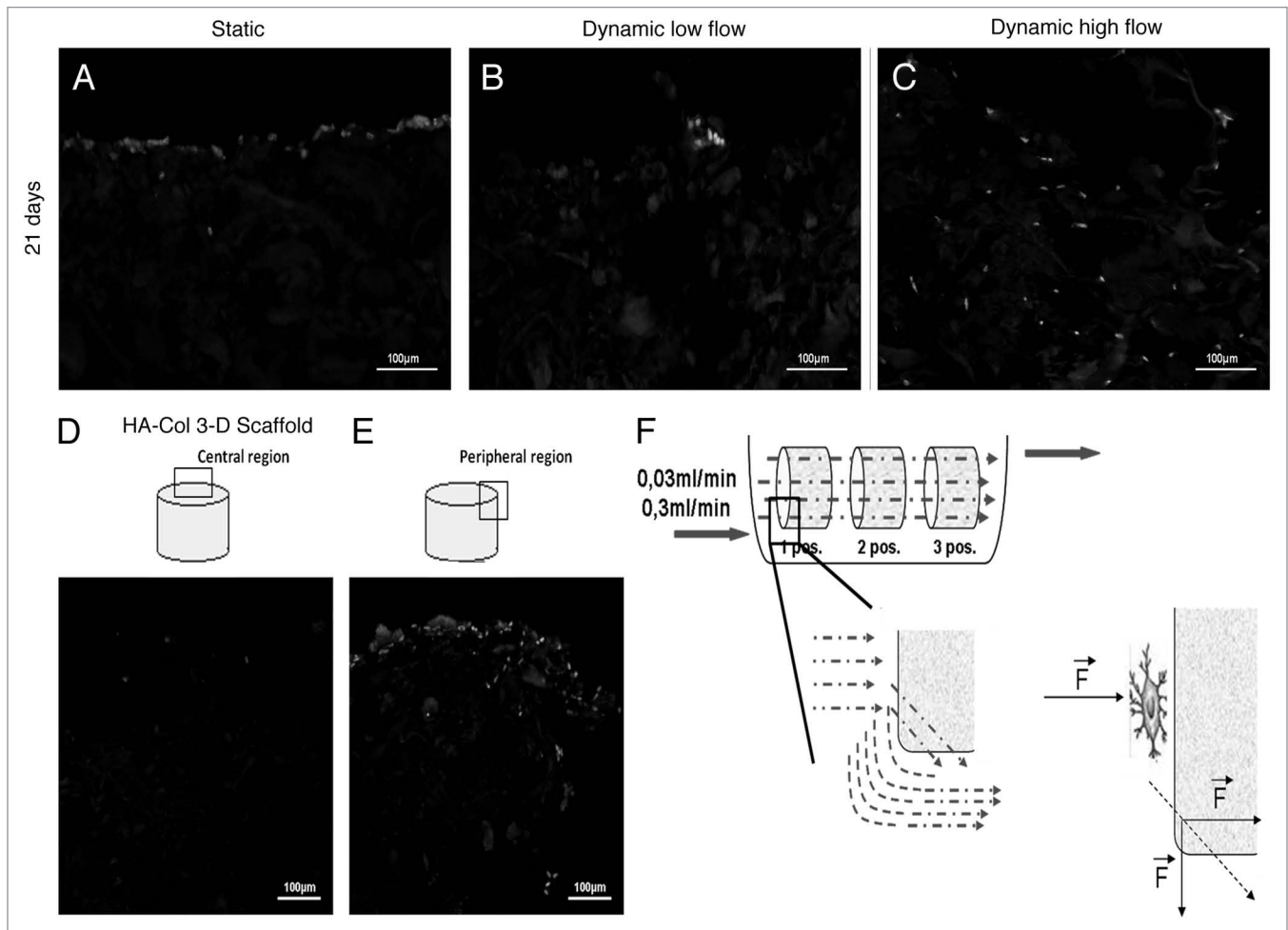


**Figure 4.** HA-Col scaffold colonization under different culture conditions after 21 d (**A, B and C**). Heterogeneity of colonization at the central (**D**) and peripheral regions (**E**) of HA-Col scaffolds under low flow-rate conditions. Scheme of fluid flow at the surface of HA-Col scaffolds within bioreactors (**F**).

times (Fig. 5B). A significantly higher viable cell number was measured at positions 1 and 3 than at position 2 after 1 d of culture. After 3 d, only position 1 presented a higher viable cell number (Fig. 5B). No more differences between positions were observed from 7 to 21 d. In contrast, few significant differences between positions were observed under high flow-rate conditions (Fig. 5C).

**Cell differentiation.** Globally, the expression of differentiation markers was higher in low flow-rate culture conditions than in the two others (Fig. 6). Alkaline phosphatase (ALP) activity increased similarly with culture time for static and low flow-rate conditions but it was 2-fold higher in low flow-rate than in static conditions after 14 and 21 d. In contrast, ALP activity in high flow-rate conditions did not change with culture time and stayed at a very low level comparable to the 7-d values for all culture conditions. The osteocalcin (OC) and type I procollagen (PICP) synthesis displayed very similar profiles with a significantly higher value after 14 d for low flow-rate and after 7 d for high flow-rate. The OC and PICP synthesis were more than 10-times higher in low flow-rate conditions than in static conditions. Comparison of low and high flow-rate conditions

showed the highest synthesis of OC and PICP for high flow after 7 d and the highest and tremendous synthesis for low flow after 14 d.

**Extracellular matrix production and calcium adsorption.** By SEM, we could observe that the cell morphology was substantially influenced by the cell culture conditions (Fig. 7). A scaffold's surface covered by cells was visualized up to 21 d in static conditions. The cells adhered and spread with formation of filopodia. When cells were submitted to a continuous medium-flow, their morphology and behavior changed. Some clusters of non-viable cells were noted on low flow-rate micrographs (Fig. 7B). These cell agglomerates appeared heterogeneously on the surface. As seen for the cell viability results, the cell death was more frequent in this condition than in the static one. Under high flow-rate conditions, we observed numerous viable cells on the surface. They were spread and showed a good interaction with the scaffold Col fibers (Fig. 7C). Some mineral and fibrous structures appeared on the cells and scaffold surface. Probably, cells started de novo extracellular matrix production. After 3 weeks, we could confirm that the increase of flow rate drastically influenced the cell behavior.

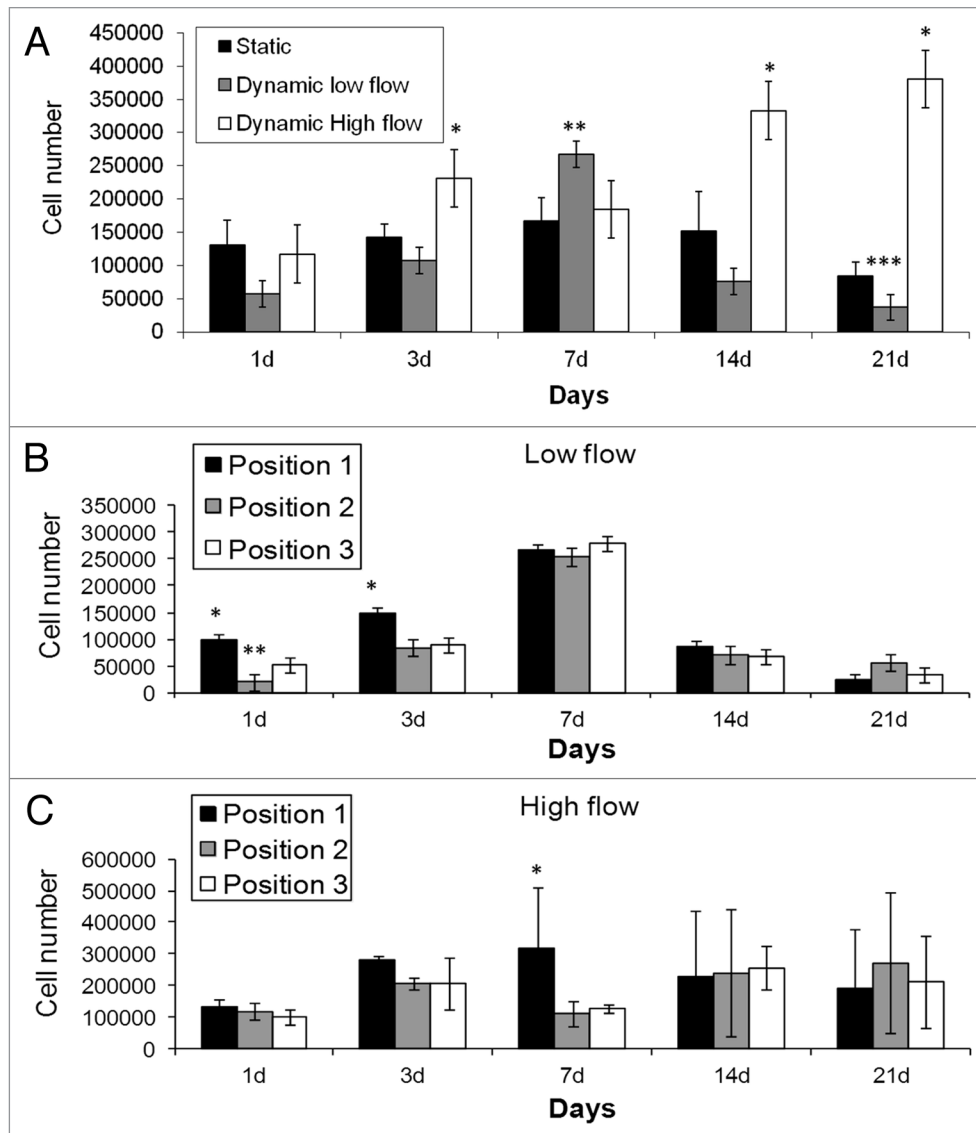


**Figure 5.** (A) Number of STRO-1A cells cultured on HA-Col scaffold under different conditions up to 21 d; (B) Number of STRO-1A cells cultured up to 21 d on HA-Col scaffold at different positions within the bioreactor under low and (C) high flow-rate. Error bars represent mean  $\pm$  SD with  $n = 6$ . The symbols (\*, \*\*, \*\*\*) indicate statistical significance within a time point ( $p < 0.05$ ).

Significant calcium ion adsorption was verified by calcium quantification in the culture medium (Fig. 7D). No significant differences were observed in static and low flow-rate conditions up to 21 d. In contrast, during all experiments, samples submitted to high flow-rate conditions presented a significantly higher calcium adsorption on the scaffold; the mineral structures observed by SEM probably correspond with this result.

## Discussion

Bioreactors have been used in tissue engineering for their capacity to improve mass transfer in large scaffolds. Moreover, the fluid flow-induced shear stress applies favorable mechanical load to stimulate osteogenic differentiation of undifferentiated cells cultured in the scaffolds.<sup>5-8,10-13</sup> In this study, we

performed a comparison of two different perfusion flow-rates in Minucells<sup>®</sup> bioreactors and their effect on the proliferation, osteogenic differentiation and cell capacity to colonise macroporous hydroxyapatite-collagen (HA-Col) scaffolds. Comparisons between different flow-rates have been reported in few studies and there are a variety of flow magnitudes applied due in part to the use of various types of cells and scaffolds.<sup>10,13,17</sup> Our comparative experiment using macroporous HA-Col scaffolds cultured in Minucells<sup>®</sup> bioreactors was therefore designed (1) to permit appropriate nutrient and waste exchanges in scaffolds of large thickness, (2) to compare two different flow rate results in terms of cell viability, proliferation and differentiation, and (3) to engineer more homogenous cellular distribution inside 3D scaffolds. HA-Col scaffolds have been demonstrated to act directly on the bone integration process when applied in vivo.<sup>1,2</sup>

Increasing cell seeding efficiency and uniform cell distribution in 3-D scaffold materials might result in decreased time for a total scaffold colonization by bone tissue after implantation, accelerating the recovery of patients.<sup>8</sup> A positive effect on cell adhesion and proliferation on 3D HA-organic composites has been observed when compared with HA or TCP ceramics.<sup>1-4,12-14</sup> When Col fibers were mineralised by calcium phosphate crystals, several improvements in cell adhesion occurred, because osteoblast-like cells are highly dependent on organic/inorganic chemical composition, micro/nano morphology and surface charge of the material.<sup>1-4</sup> Similarly, we observed an excellent adhesion of STRO-1A cells on mineralised Col fibers<sup>4</sup> and the adequate macroporosity of HA-col scaffolds (Fig. 1) allowed colonization by cells when submitted to dynamic perfusion culture. The HA-Col scaffolds studied here had a relatively large pore size (mean size:  $280 \pm 80 \mu\text{m}$ ) and presented high stability under cell culture condition (Fig. 2A).

The perfusion bioreactor provides nutrient, gas and waste exchanges by liquid displacement. The enhanced mass transfer not only in the peripheral regions but also within internal pores of scaffolds has been shown to improve cellular viability in the material.<sup>6,8,10,15</sup> This was confirmed in our experiment. By MTT assay, a higher content of viable cells was observed within the two dynamic conditions compared with statically cultured scaffolds up to 7 d (Fig. 5A). However, on days 14 and 21, highly significant differences were observed in cell proliferation under high perfusion flow-rate compared with the low flow-rate. The number of cells submitted to low flow-rate decreased drastically on day 21 and became even significantly lower than in scaffolds cultured statically (Fig. 5A). Moreover, bioreactor sample position appeared to be a determinant of cell viability at the initial time-points (Fig. 5B, C). For the first 3 d, the bioreactor position 1 showed enhanced viable cell number compared with the two other positions under low perfusion flow-rate (Fig. 5B). This confirmed that differences in magnitude, orientation, continuous or intermittent flow-displacement applied at specific location in a perfusion bioreactor are important factors for cell viability.<sup>6,10</sup> Depending of stress magnitude, signal intracellular pathway might generate positive or negative contribution to cell viability. Scaffold placed at position 2 within bioreactor chamber may be exposed to different fluid-induced shear than at positions 1 and 3, which could cause lower cell viability. For high flow-rates (0.3 mL/min), cell density was independent of the sample position inside the bioreactor demonstrating that transfer mass convection was able to establish a uniform perfusion (Fig. 5C).

Cell number and spatial cellular distribution in HA-Col scaffolds were also investigated by histology. Scaffolds cultured in static conditions presented uniform multilayers of cells on their external surface, a phenomenon that was lessened in perfusion culture (Fig. 4A). Thus, the limitations in diffusion and mass transport in static conditions resulted in an encapsulation effect, in accordance with previous publications.<sup>5-8</sup> In the low perfusion flow-rate culture, a few isolated cells were seen on the surface and a significant decrease of total cell nuclei number was observed (Fig. 4B). Moreover, these cells exhibited morphological signs of necrosis (Fig. 7B). In contrast, under high perfusion flow-rate

condition, cells had infiltrated further into the center of HA-Col scaffolds up to 21 d (Fig. 4C). This may indicate that cells are sensitive to minimal shear stresses and have a preferential migration toward the center of the scaffold when sufficient levels of nutrients/oxygen and removal of inhibitory waste products allow increased cell viability and scaffold colonization.<sup>10</sup> As seen in Figure 4D and E, cells colonized HA-Col scaffolds preferentially from peripheral regions in contrast to the results of Volkmer et al.<sup>15</sup> According to David et al. (2011), peripheral regions of scaffolds cultured under indirect perfusion systems - where the scaffold is not tightly sealed to the bioreactor - present more elevated convection currents, with a higher magnitude force, resulting in a preferential cell distribution.<sup>10</sup> Janssen et al. have reported differences in biophysical forces induced by fluid flow displacement between direct and indirect perfusion bioreactors.<sup>8</sup> Systems using direct perfusion have been shown to enhance cell density in the central region of scaffolds differently to indirect perfusion ones. Effectively, in our system, medium flow passes the path of least resistance around the scaffold and only partly through it, justifying the cell presence at peripheral regions (Fig. 4F). Additionally, Zhang et al. asserted that cells at the frontal zones are washed away by the oncoming perfusion flow with high flow-rates.<sup>3</sup> In our study, both flow rates presented lower cell nuclei distribution in the central scaffold regions (Fig. 4D, E). We believe that, beside lower nutrients/oxygen supply and inhibitory waste products removal in these regions, unquantifiable physical disturbances, such as shear and normal stresses, could induce cellular damage and disrupt cellular attachment as previously observed.<sup>10</sup>

A more homogenous distribution of cells would be preferable before in vivo implantation of tissue engineering constructs, because a high cell quantity would enhance cell differentiation and matrix deposition.<sup>6,11</sup> The differentiation of cells toward an osteogenic lineage also depends on a high confluence of cells inside scaffolds as cell-cell contacts are needed for differentiation. Moreover, the increase in extracellular matrix deposition has been demonstrated to be influenced by mechanotransduction due to perfusion shear stresses.<sup>5,10-13</sup> Our results show that bioreactor culture significantly enhanced expression of alkaline phosphatase (ALP), osteocalcin (OC) and pro-collagen type I (PIP) compared with scaffolds cultured in static conditions (Fig. 6). These results indicate that shear stresses induced an earlier osteogenesis, as previously shown by other studies.<sup>6,10,13</sup> However, osteogenic markers were not upregulated in higher perfusion flow-rate culture (0.3 mL/min; Figure 6). ALP expression generally increases after the proliferation phase and is involved in the early initiation of the mineralization process.<sup>13</sup> This could explain the significant increase in the ALP level that we observed on days 14 and 21 under both low perfusion flow-rate and static culture, while cells no longer proliferated and were concentrated in external regions of the scaffold. However, if shear stress exceeds a certain limit, ALP activity can be downregulated as we observed (Fig. 6A).<sup>5</sup> Our OC results under static culture are in agreement with the differentiation and maturation proposition where cells present upregulated osteogenic markers after confluence and when cell-cell contacts are formed. On the contrary,

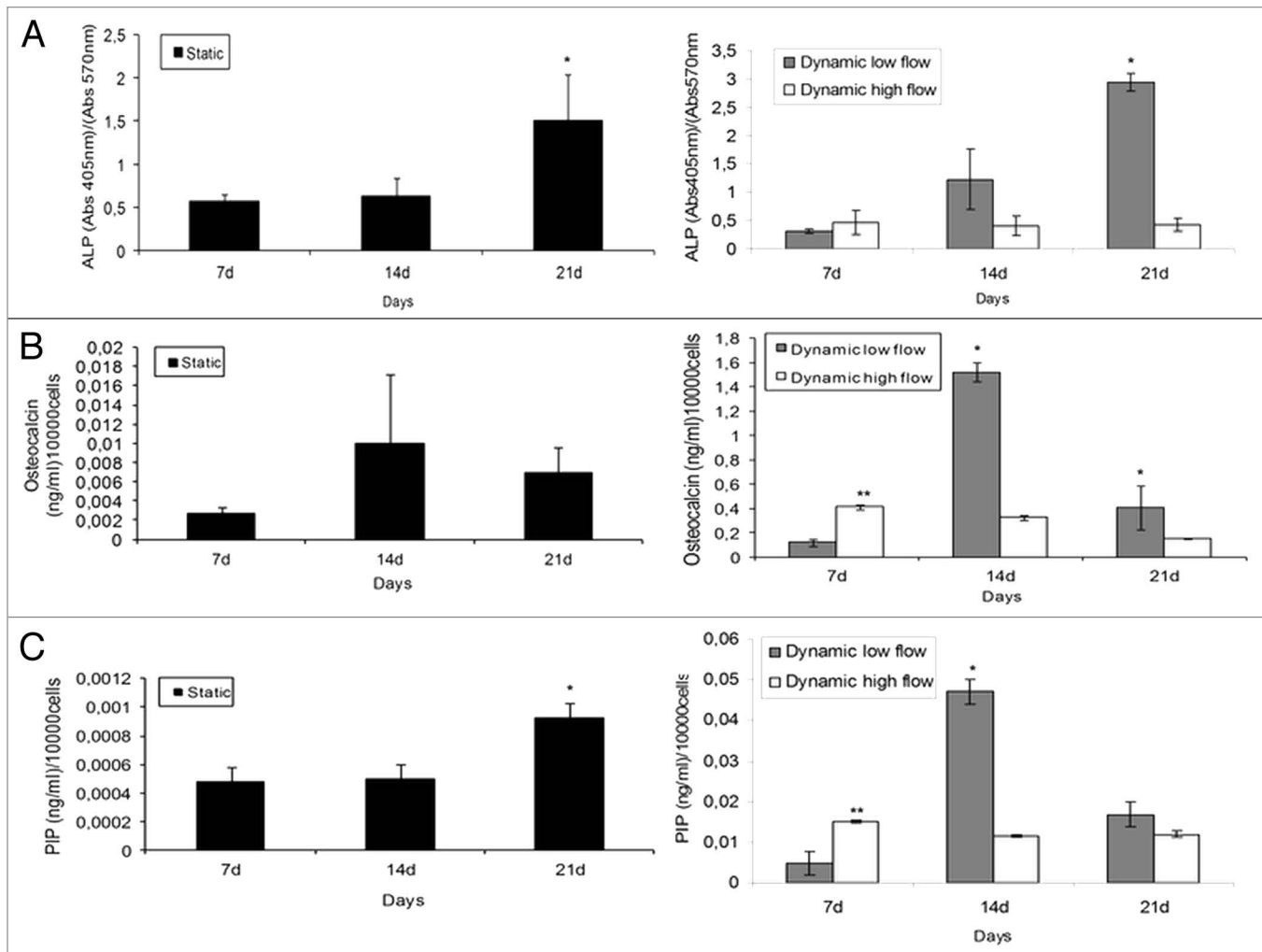


**Figure 6.** Alkaline phosphatase (ALP) (A), osteocalcin (OC) (B) and pro-collagen I (PIP) (C) production by STRO-1A cells cultured on 3D cross-linked HA-Col scaffold up to 21 d under static and dynamic conditions. Error bars represent means  $\pm$  SD for  $n = 3$ . The symbols (\*, \*\*) indicate statistical significance within a timepoint and a culture condition ( $p < 0.05$ ).

a significant decrease in osteocalcin synthesis was observed between day 7 and 21 under high perfusion flow-rate (Fig. 6B). Some authors have demonstrated that mechanical stresses exerted in dynamic cultures could result in downregulation of osteocalcin expression or later cell differentiation process.<sup>11</sup> Even if higher levels of PIP were expressed by STRO-1A cells under a low perfusion flow-rate system compared with a static one, an insignificant expression was noted with high flow-rate culture (Fig. 6C). PIP is known to be expressed during culture and to be gradually downregulated throughout osteoblast differentiation and maturation. The higher PIP levels observed on days 14 and 21 (in low perfusion flow-rate and static culture, respectively) confirmed a late STRO-1A maturation (Fig. 6C).

For the high perfusion flow-rate system (0.3 mL/min), it can be speculated that: (1) STRO-1A cells were still in an active proliferative phase because cells are still in a continuous scaffold colonization process; (2) high flow-perfusion-rate and a closed perfusion circuit resulted in abundant amounts of proteins deposited on the organic/inorganic matrix;<sup>5</sup> and, (3) a HA-Col

scaffold degradation may also occur under higher flow-rate.<sup>16</sup> High perfusion flow-rate culture presented a significantly lower  $Ca^{+2}$  ion concentration in the culture medium than in the other two culture systems. This illustrates a strong calcium adsorption on the scaffolds that could be accompanied, at the same time, by capture of OC and PIP molecules in the mineral deposits on the extracellular matrix formed by STRO-1A cells on the scaffold because of the close perfusion system used with high perfusion flow-rate. Indeed, osteocalcin has a strong affinity for calcium phosphate and is able to control in vitro and in vivo the alkaline phosphatase-induced mineralization of collagen.<sup>18-21</sup>

Finally, the present study established that different perfusion flow-rates provide a variable environment for STRO-1A cell proliferation and differentiation. The macroporous HA-Col scaffolds were able to support cell proliferation and colonization only under high perfusion flow-rate. In contrast, low perfusion flow-rate data confirmed that appropriate oxygen transport, waste removal and shear stresses are essential parameters to obtain cell viability suitable for tissue engineering applications.



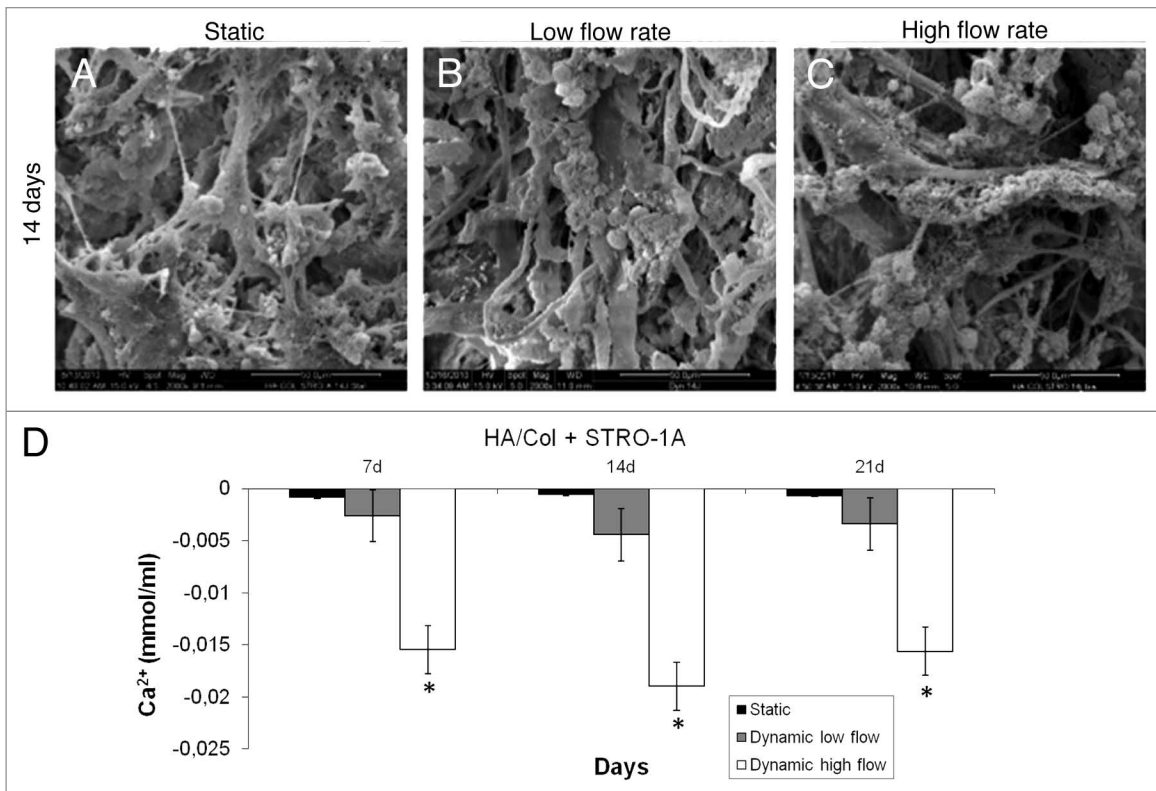


**Figure 7.** SEM micrographs of STRO-1A cells cultured on 3D cross-linked HA-Col scaffolds during 14 d under static (A), low flow rate (B) and high flow rate (C) dynamic conditions. Bar = 50  $\mu$ m, original magnification: 2000x. Calcium adsorption on HA-Col scaffold matrix under different conditions up to 21 d (D). Error bars represent mean  $\pm$  SD with  $n = 6$ . The symbol (\*) indicates statistical significance within a timepoint ( $p < 0.05$ ).

Moreover, comparison of open (low flow) and closed circuit (high flow) suggested a possible adsorption of synthesized biomolecules such as osteocalcin and collagen on HA-Col scaffold in the closed circuit.

## Materials and Methods

**HA-Col scaffold fabrication.** The scaffolds were prepared as previously described.<sup>4</sup> Briefly, isolation of collagen (Col) fibrils from bovine Achilles tendon was performed by the enzymatic action of pepsin (Sigma-Aldrich, ref. P7000) in a 0.5 M acetic acid solution (Merck, ref. 109951) up to 24 h at 37°C. The extraction solution was centrifuged at 90,000 g (Eppendorf, ref. 5810R) for complete removal of impurities. The Col fibers were precipitated by 10% NaCl solution (Vetec, ref. 1543). The precipitated fibers were dialysed in distilled water for 3 d and redissociated in 59.32 mM orthophosphoric acid (Merck, ref. 100573). The final fiber solution (at a concentration of 12 mg/mL) was stored at 4°C until use. The HA/Col (50:50 wt%) 3D scaffolds were prepared by simultaneously dropping 59.32 mM orthophosphoric acid solution (containing the Col fibrils) and 37.2 mM calcium nitrate (Merck, ref. 102120) solution into a flask containing double-distilled water. The temperature and pH were adjusted to 38°C and 9, respectively. After the complete addition of the two solutions, the material was maintained under synthesis conditions for 3 h. The synthesized composites were cross-linked by 0.125%

glutaraldehyde (TedPella, ref. 18427) solution, poured in cylindrical molds (4-mm diameter and 3-mm high) and lyophilised for 48 h. Finally, the scaffold samples presenting the theoretical Ca/P ratio of 1.67 were sterilised with a total dose of 25 kGy using  $\gamma$  radiation.

**HA-Col scaffold characterization. Scaffold porosity.** Scaffold samples were fixed with 10% neutral-buffered formalin solution (Fisher Scientific, ref. 10010150) for 24 h. Standard dehydration in ethanol solutions sequentially increasing to 100% ethanol (Fisher Scientific, ref. 10007731) was performed followed by immersion in xylene (Fisher Scientific, ref. 10385910), paraffin-saturated xylene and finally molten paraffin (Fisher Scientific, ref. 10395900). Blocks were cut in 15- $\mu$ m thick sections that were stained by Picrosirius solution. Images of these sections were acquired using an Olympus BX 51 microscope. The HA-Col scaffold porosity percentage and mean pore width were measured on these images using Image J 1.45s software (National Institute of Mental Health, Bethesda, Maryland, USA). The porosities were calculated on sections following two different directions: (1) 15 random images of ten serial cross-sections parallel to the surface on two scaffolds; and (2) 50 random images (for each condition and endpoint) distributed evenly throughout cross-sections perpendicular to the surface of HA-Col scaffolds submitted to different conditions of culture up to 21 d.

**Scaffold permeability.** The permeability of cross-linked HA-Col scaffolds ( $n = 4$ ) was determined from the hexane

liquid displacement (Hexane 99%, Spectrosol, Sigma-Aldrich ref. 139386). Hexane has the ability to penetrate the matrix without deforming it. Scaffold samples ( $n = 3$ ) with the same height were inserted in the initial volume ( $V1$ ) of hexane column and maintained for 300 sec. The HA-Col permeability was calculated from Eqn. 1:

$$\varepsilon(\%) = (V1 - V3)/(V2 - V3) \times 100 \quad (1)$$

where  $V1$  is the initial hexane volume,  $V2$  is the total volume (hexane + scaffold up to 300 sec) and  $V3$  is the residual hexane volume after material removal.

**Scaffold microstructure.** The microstructure of the cross-linked HA-Col scaffolds was observed by scanning electron microscopy (SEM). The 3D scaffolds were fixed with glutaraldehyde (4%) and paraformaldehyde (2%) (Sigma-Aldrich ref. 158127) in phosphate-buffered saline (PBS; pH 7.4). They were dehydrated in increasing ethanol solutions (50, 70, 80, 95 and 100%) and immersed twice for 10 min in each solution. After complete dehydration using hexamethyldisilazane (HMDS; Sigma-Aldrich, ref. 379212), the scaffolds were gold-coated and examined under a Quanta 400 environmental scanning electron microscope (FEI).

**HA-Col scaffold colonization. STRO-1A cell culture.** Immortalised human stromal cells (STRO-1A)<sup>22</sup> were kindly provided by P. Marie (Inserm U606, Paris, France). When STRO-1A cells had reached confluence, they were detached with trypsin-ethylenediamine tetra-acetic acid (trypsin-EDTA, Sigma-Aldrich T4049), counted and re-suspended in culture medium (Iscove's medium (Sigma-Aldrich I3390) with L-glutamine (Sigma-Aldrich G7513) containing 10% fetal bovine serum (VWR BWSTS1810/100), 100 U/mL penicillin G (Sigma-Aldrich P3032), 100  $\mu$ g/mL streptomycin sulfate (Sigma-Aldrich S9137) and  $10^{-8}$  M dexamethasone (Sigma-Aldrich D4902).

**Inoculation of scaffolds and static culture.** The sterilised scaffolds were rehydrated with complete cell culture medium for 24 h before cell culture. After this period, STRO-1A cells were seeded onto the porous scaffolds by adding 50  $\mu$ L of cell suspension media to scaffolds (seeding density  $5 \times 10^5$  cells/scaffold), placed in 24-well culture plates and incubated for 30 min in an incubator. Thereafter, 2 mL of Iscove's medium was slowly added to each well and STRO-1A cells were incubated in a humidified atmosphere at 37°C and 5% CO<sub>2</sub> for 24 h (to allow the initial cellular attachment on the scaffolds). The inoculated scaffolds were further cultured under static condition for 24 h and 3, 7, 14 and 21 d in a humidified incubator at 37°C and 5% CO<sub>2</sub>. The medium was renewed three times per week.

**Dynamic cultures.** The dynamic culture condition was applied within perfusion bioreactors supplied by Minucells and Minutissue™ (Bad Abbach, ref. 1307). This perfusion system, which allows perfusion of up to six scaffolds in parallel depending on their size, is connected to an open circuit meaning that the container is connected to a medium bottle (input) and to a waste reservoir (output) by gas-permeable silicon tubes. The STRO-1A cells seeded on the HA-Col scaffolds were maintained for 24 h in static condition to allow total cell adhesion. Then, samples were placed in the perfusion container within

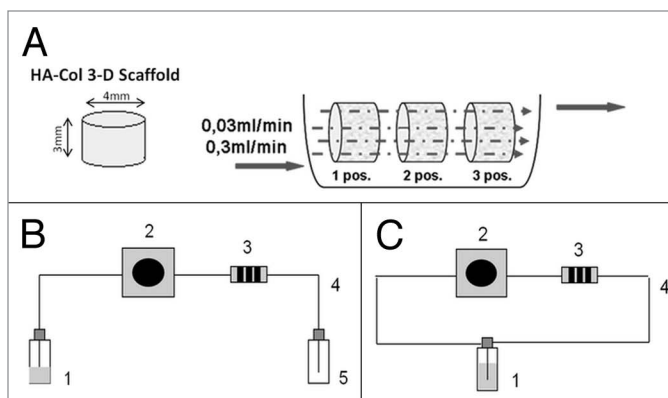


**Figure 8.** Schematic diagram of three HA-Col scaffolds submitted to two dynamic environments within the perfusion bioreactor (A). Scheme of the open circuit with low flow-rate (0.03 mL/min); (B) and the closed circuit with high flow-rate (0.3 mL/min); (C) 1 and 5, medium flasks; 2, peristaltic pump; 3, bioreactor; 4, gas-permeable silicon connecting tubes.

which they were separated by support rings and cultured for 1, 3, 7, 14 and 21 d at a temperature of 37°C and a carbon dioxide concentration of 5%. Only three samples were put in each bioreactor considering their size and to reduce the risk of hypoxia. Two constant flow perfusion rates at 0.03 (2) and 0.3 mL/min (20 mL/h)—low and high flow-rate respectively—were applied (Fig. 8A). For the low flow, the open circuit was maintained although it was closed for the high flow due to medium cost (Fig. 8B, C). In the low-flow condition, 250 mL of medium circulated in the bioreactor and was renewed every three/four days while in the high-flow condition, 250 mL of medium circulated in the bioreactor and was renewed every seven days. Cultures were maintained for up to 21 d.

**Cell viability.** The viability of STRO-1A cells cultured on HA-Col scaffolds was determined using the MTT (3-{4,5-dimethylthiazol-2-yl}-2,5-diphenyl-2H-tetrazolium-bromide; Sigma-Aldrich, ref M5655) assay. The samples ( $n = 6$ ) were incubated in 500  $\mu$ L of MTT solution (0.5 mg/mL) at 37°C in a humidified atmosphere containing 5% CO<sub>2</sub> for 3 h. After the complete withdrawal of MTT, 500  $\mu$ L of acidic isopropanol (0.3%) (Sigma-Aldrich W292907) was added to the samples for 10 min. The optical density of the acidic isopropanol was read at 570 nm on a microplate reader (ELX, 800UV, Biotec Instruments, INC).

**Cell colonization.** The capacity of the STRO-1A cells to colonise the scaffold up to 21 d after inoculation was analyzed by cell nuclei visualization and quantification on histological cross-sections ( $n = 4$ ) using Image J 1.45s software (National Institute of Mental Health, Bethesda, Maryland, USA). For this, the scaffolds were embedded in paraffin as previously described. Blocks were sectioned perpendicular to the surface at a thickness of 15  $\mu$ m using a microtome and sections were stained with 4',6'-diamidino-2-phenylindole dihydrochloride (DAPI; Sigma-Aldrich, ref D8417) for the visualization of cell nuclei. Digital images were acquired using an Olympus BX51-P microscope.

**Cell differentiation.** Alkaline phosphatase (ALP) activity was measured in culture medium using p-nitrophenylphosphate (PnPP, Sigma-Aldrich, ref PS613) as substrate in an alkaline buffer solution (20 mM p-nitrophosphate PnP + 100 mM diethanolamine 98% + 10 mM MgCl<sub>2</sub>, pH 9.5 at room temperature). The scaffolds (n = 6) were permeabilised with a 0.5% aqueous solution of Triton X-100 (Sigma-Aldrich, ref T9284) and incubated for 30 min at 37°C with the substrate (PnPP). Then, the reaction was terminated with the addition of EDTA solution (0.1 M EDTA in 1 M NaOH solution) (Sigma-Aldrich, ref E6758). The optical density of the solution was read on a plate reader at 405 nm.

The osteocalcin (OC) and pro-collagen (PIP) concentrations were measured using the ELISA method and the Gla-type Osteocalcin and Procollagen Type I C-peptide EIA commercial kits, respectively (Bio Inc. TANAKA., ref MK111 and MK101, respectively). The medium samples were inoculated in the labeling microplates (96 wells) coated with specific immobilised enzymes. The experiment was conducted in triplicate and repeated two times (n = 6). The substrate reaction was calculated by colorimetric measurements at 450 nm. The intensity of the solution was proportional to the OC and PIP concentrations secreted by the STRO-1A cells in the medium samples.

## References

1. Itoh S, Kikuchi M, Koyama Y, Takakuda K, Shinomiya K, Tanaka J. Development of an artificial vertebral body using a novel biomaterial, hydroxyapatite/collagen composite. *Biomaterials* 2002; 23:3919-26; PMID:12162324; [http://dx.doi.org/10.1016/S0142-9612\(02\)00126-6](http://dx.doi.org/10.1016/S0142-9612(02)00126-6).
2. Tcacencu I, Wendel M. Collagen-hydroxyapatite composite enhances regeneration of calvaria bone defects in young rats but postpones the regeneration of calvaria bone in aged rats. *J Mater Sci Mater Med* 2008; 19:2015-21; PMID:17952564; <http://dx.doi.org/10.1007/s10856-007-3284-2>.
3. Zhang L, Tang P, Xu M, Zhang W, Chai W, Wang Y. Effects of crystalline phase on the biological properties of collagen-hydroxyapatite composites. *Acta Biomater* 2010; 6:2189-99; PMID:20040387; <http://dx.doi.org/10.1016/j.actbio.2009.12.042>.
4. Campos DM, Anselme K, Soares GDD. In Vitro Biological Evaluation of 3-D Hydroxyapatite/Collagen (50/50 wt. (%)) Scaffolds. *Mater Res* 2012; 15:151-8; <http://dx.doi.org/10.1590/S1516-14392011005000099>.
5. Rauh J, Milan F, Günther KP, Stiehl M. Bioreactor systems for bone tissue engineering. *Tissue Eng Part B Rev* 2011; 17:263-80; PMID:21495897; <http://dx.doi.org/10.1089/ten.teb.2010.0612>.
6. Martin I, Wendt D, Heberer M. The role of bioreactors in tissue engineering. *Trends Biotechnol* 2004; 22:80-6; PMID:14757042; <http://dx.doi.org/10.1016/j.tibtech.2003.12.001>.
7. Bancroft GN, Sikavitsas VI, Mikos AG. Design of a flow perfusion bioreactor system for bone tissue-engineering applications. *Tissue Eng* 2003; 9:549-54; PMID:12857422; <http://dx.doi.org/10.1089/107632703322066723>.
8. Jansen FW, Oostra J, Oorschot Av, van Blitterswijk CA. A perfusion bioreactor system capable of producing clinically relevant volumes of tissue-engineered bone: in vivo bone formation showing proof of concept. *Biomaterials* 2006; 27:315-23; PMID:16125223; <http://dx.doi.org/10.1016/j.biomaterials.2005.07.044>.

**Calcium ions absorption.** Ca<sup>2+</sup> ion concentration was obtained in culture medium using an arsenate III commercial kit (DiaSys, EC, ref. 111819910704). To obtain the calcium ion concentration in the medium samples, the color of the solution was measured by a microplate reader at 650 nm (ELX, 800UV, Biotech Instruments, Inc.). Data represent the mean ± SE from six wells for each condition.

**Statistical analysis.** Quantitative data are presented as mean ± standard deviation (SD). After the Shapiro-Wilk normality test, ANOVA (one-way) and Tukey post-hoc tests were performed to determine the statistical significance between experimental groups. A value of p < 0.05 and p < 0.01 were considered to be statistically significant.

## Disclosure of Potential Conflicts of Interest

No potential conflicts of interest were disclosed.

## Acknowledgments

The authors would like to thank FAPERJ, CNPq and the CAPES-COFECUB project n° 628/09 for financial support.

9. Chu XH, Shi XL, Feng ZQ, Gu JY, Xu HY, Zhang Y, et al. In vitro evaluation of a multi-layer radial-flow bioreactor based on galactosylated chitosan nanofiber scaffolds. *Biomaterials* 2009; 30:4533-8; PMID:19500837; <http://dx.doi.org/10.1016/j.biomaterials.2009.05.020>.
10. David B, Bonnefont-Rousselot D, Oudina K, Degat MC, Deschepper M, Viateau V, et al. A perfusion bioreactor for engineering bone constructs: an in vitro and in vivo study. *Tissue Eng Part C Methods* 2011; 17:505-16; PMID:21171934; <http://dx.doi.org/10.1089/ten.tec.2010.0468>.
11. Yeatts AB, Fisher JR. Tubular perfusion system for the long-term dynamic culture of human mesenchymal stem cells. *Tissue Eng Part C Methods* 2011; 17:337-48; PMID:20929287; <http://dx.doi.org/10.1089/ten.tec.2010.0172>.
12. Wang YC, Uemura T, Dong J, Kojima H, Tanaka J, Tateishi T. Application of perfusion culture system improves in vitro and in vivo osteogenesis of bone marrow-derived osteoblastic cells in porous ceramic materials. *Tissue Eng* 2003; 9:1205-14; PMID:14670108; <http://dx.doi.org/10.1089/10763270360728116>.
13. Uemura T, Dong J, Wang Y, Kojima H, Saito T, Iejima D, et al. Transplantation of cultured bone cells using combinations of scaffolds and culture techniques. *Biomaterials* 2003; 24:2277-86; PMID:12699664; [http://dx.doi.org/10.1016/S0142-9612\(03\)00039-5](http://dx.doi.org/10.1016/S0142-9612(03)00039-5).
14. Bernhardt A, Lode A, Boxberger S, Pompe W, Gelinsky M. Mineralised collagen—an artificial, extracellular bone matrix—improves osteogenic differentiation of bone marrow stromal cells. *J Mater Sci Mater Med* 2008; 19:269-75; PMID:17597360; <http://dx.doi.org/10.1007/s10856-006-0059-0>.
15. Volkmer E, Drosse I, Otto S, Stangelmayer A, Stengele M, Kallukalam BC, et al. Hypoxia in static and dynamic 3D culture systems for tissue engineering of bone. *Tissue Eng Part A* 2008; 14:1331-40; PMID:18601588; <http://dx.doi.org/10.1089/ten.tea.2007.0231>.
16. Meinel L, Karageorgiou V, Fajardo R, Snyder B, Shinde-Patil V, Zichner L, et al. Bone tissue engineering using human mesenchymal stem cells: effects of scaffold material and medium flow. *Ann Biomed Eng* 2004; 32:112-22; PMID:14964727; <http://dx.doi.org/10.1023/B:ABME.000007796.48329.b4>.
17. Grayson WL, Bhumiratana S, Cannizzaro C, Chao PH, Lennon DP, Caplan AI, et al. Effects of initial seeding density and fluid perfusion rate on formation of tissue-engineered bone. *Tissue Eng Part A* 2008; 14:1809-20; PMID:18620487; <http://dx.doi.org/10.1089/ten.tea.2007.0255>.
18. Doi Y, Horiguchi T, Kim SH, Moriwaki Y, Wakamatsu N, Adachi M, et al. Effects of non-collagenous proteins on the formation of apatite in calcium beta-glycero-phosphate solutions. *Arch Oral Biol* 1992; 37:15-21; PMID:1596204; [http://dx.doi.org/10.1016/0003-9969\(92\)90147-Z](http://dx.doi.org/10.1016/0003-9969(92)90147-Z).
19. Fujisawa R, Kuboki Y. Affinity of bone sialoprotein and several other bone and dentin acidic proteins to collagen fibrils. *Calcif Tissue Int* 1992; 51:438-42; PMID:1451011; <http://dx.doi.org/10.1007/BF00296677>.
20. Roy ME, Nishimoto SK. Matrix Gla protein binding to hydroxyapatite is dependent on the ionic environment: calcium enhances binding affinity but phosphate and magnesium decrease affinity. *Bone* 2002; 31:296-302; PMID:12151082; [http://dx.doi.org/10.1016/S8756-3282\(02\)00821-9](http://dx.doi.org/10.1016/S8756-3282(02)00821-9).
21. Fujisawa R, Tamura M. Acidic bone matrix proteins and their roles in calcification. *Front Biosci* 2012; 17:1891-903; PMID:22201843; <http://dx.doi.org/10.2741/4026>.
22. Oyajobi BO, Lomri A, Hott M, Marie PJ. Isolation and characterization of human clonogenic osteoblast progenitors immunoselected from fetal bone marrow stroma using STRO-1 monoclonal antibody. *J Bone Miner Res* 1999; 14:351-61; PMID:10027900; <http://dx.doi.org/10.1359/jbmr.1999.14.3.351>.